Provided for non-commercial research and education use.
Not for reproduction, distribution or commercial use.

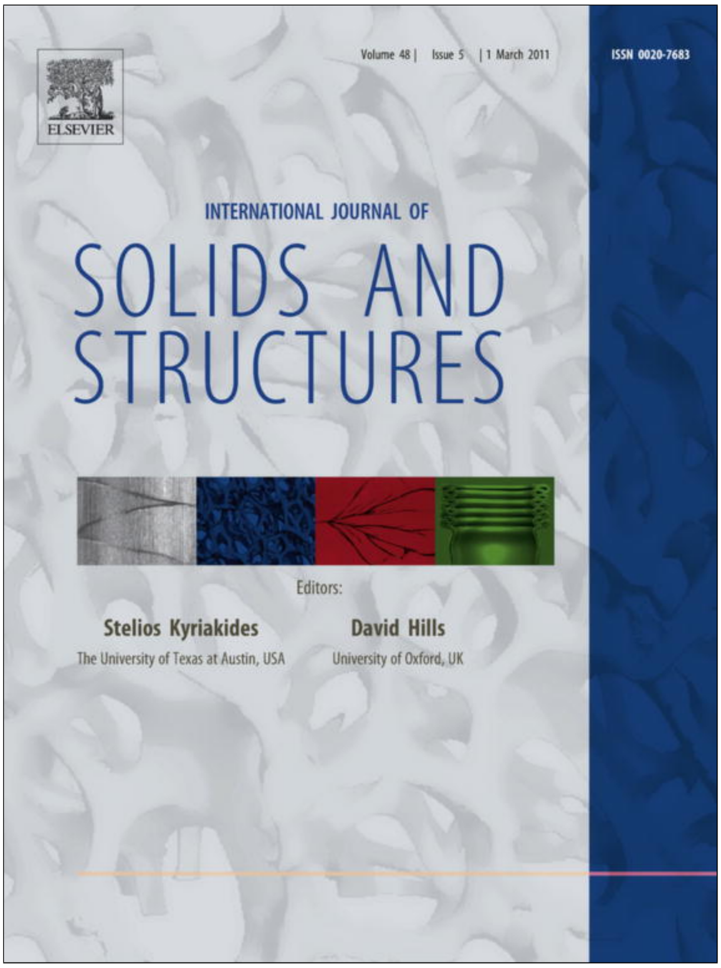

Volume 48 | Issue 5 | 1 March 2011
ISSN 0020-7683
ELSEVIER

INTERNATIONAL JOURNAL OF
SOLIDS AND STRUCTURES

Editors:
Stelios Kyriakides
The University of Texas at Austin, USA
David Hills
University of Oxford, UK

This article appeared in a journal published by Elsevier. The attached copy is furnished to the author for internal non-commercial research and education use, including for instruction at the authors institution and sharing with colleagues.

Other uses, including reproduction and distribution, or selling or licensing copies, or posting to personal, institutional or third party websites are prohibited.

In most cases authors are permitted to post their version of the article (e.g. in Word or Tex form) to their personal website or institutional repository. Authors requiring further information regarding Elsevier's archiving and manuscript policies are encouraged to visit:

http://www.elsevier.com/copyright

International Journal of Solids and Structures 48 (2011) 673–679

Contents lists available at ScienceDirect

International Journal of Solids and Structures

journal homepage: www.elsevier.com/locate/ijsolstr

A general perturbation method for inhomogeneities in anisotropic and piezoelectric solids with applications to quantum-dot nanostructures

H.J. Chu [a,b], E. Pan [b,*], J.J. Ramsey [b], J. Wang [c], C.X. Xue [b,d]

[a] *College of Hydraulic Science and Engineering, Yangzhou University, Yangzhou 225009, PR China*
[b] *Department of Civil Engineering, University of Akron, Akron 44311, USA*
[c] *Department of Mechanics and Aerospace Engineering, College of Engineering, Peking University, Beijing 100871, PR China*
[d] *Department of Mechanics, College of Science, North University of China, Taiyuan 030051, PR China*

ARTICLE INFO

Article history:
Received 7 May 2010
Received in revised form 25 August 2010
Available online 11 November 2010

Keywords:
Quantum dot
Nanostructure
Anisotropic
Piezoelectric
Perturbation theory

ABSTRACT

By introducing a homogeneous piezoelectric material and its Green's function, we present a new semi-analytical three-dimensional perturbation method for general inhomogeneity problems in anisotropic and piezoelectric solids. This method removes the limitations associated with previous analytical methods, which often ignore the anisotropic properties or the difference between the material properties of the inhomogeneity and its surrounding matrix. As an important application, the proposed theory is employed to calculate the elastic and electric fields in a truncated pyramidal InAs/GaAs quantum-dot (QD) nanostructure. Numerical results demonstrate that the anisotropy of the materials and the difference between the material constants of the QD and the matrix have a significant influence on the strain and electric fields. The relative differences of the strain and electric field inside the QD between the simplified isotropic and homogeneous model and the real anisotropic and heterogeneous one may reach 22% and 53%, respectively. The accuracy of the calculated elastic strain and electric fields is improved greatly by a second order approximate solution (OAS). Since the third OAS nearly coincides with the second one, good convergence of the iteration procedure is demonstrated. Moreover, contours of the hydrostatic strain and electric potential within and around the QD are also presented and analyzed.

© 2010 Elsevier Ltd. All rights reserved.

1. Introduction

Inhomogeneities in solids are of great interest. Particularly in recent years, considerable efforts have been invested in the study of semiconductor nanostructures such as quantum wells (QWs), quantum wires (QWRs), and quantum dots (QDs) due to their special physical behaviors (Bandyopadhyay and Nalwa, 2003; Steiner, 2004; Wang and Voliotis, 2006; Cullis and Midgley, 2008; Duggen et al., 2008; Shih et al., 2009). Because of the difference between material properties of the inhomogeneity and its surroundings in a QD or QWR structure, lattice or thermal mismatch often plays an outstanding role in the fabrication of these nanostructures (Holý et al., 1999; Heidemeyer et al., 2003; Beck et al., 2004; Pan et al., 2009; Even, 2009). Elastic strain fields are often coupled with other physical properties in semiconductor nanostructures (Widmann et al., 1998; Sharma and Ganti, 2004; Romanov et al., 2006; Garg et al., 2009; Shi et al., 2009; Zhang et al., 2009). For instance, semiconductor materials such as GaN, GaAs, InAs, and InN are often piezoelectric. Therefore, coupling between elastic strains and electric fields exists inherently in these nanostructures, i.e. the strain field induced by the lattice or thermal mismatch in nanostructures of these materials will induce an electric field, and *vice versa* (Yang, 2006; Pan et al., 2007). The relaxation of the misfit strain and consequent electric field inside a piezoelectric nanodevice may change its electronic states and band gaps (Ambacher et al., 1999; Ma et al., 2007; Lassen et al., 2008; Kurdi et al., 2010). Because strain has such a material effect on these nanostructures, accurate methods of predicting the strain in nanostructures and its effects on their properties are useful.

Distributions of elastic and electric fields, due to buried nano-inhomogeneities with misfit strains induced by lattice or thermal mismatch, can be calculated by several approaches including experimental techniques (Wang and Voliotis, 2006; Feneberg et al., 2006; Capellini et al., 2010), finite element and difference methods (FEM/FDM) (Faux et al., 1994; Liao et al., 1999; Benabbas et al., 1999; Johnson and Freund, 2001), boundary element methods (BEMs) (Yang and Pan, 2002; Pan et al., 2005), and atomistic simulations (Migliorato et al., 2002a,b; Rodríguez-López et al., 2004; Makeev et al., 2004; Gates et al., 2005; Pyrz, 2008). Atomistic simulations are, of course, far more computationally expensive compared to those employing continuum mechanics, such as FEM and BEM (Ramsey et al., 2008).

---

* Corresponding author. Tel.: +1 3309726739; fax: +1 3309726020.
E-mail addresses: hjchu@yzu.edu.cn (H.J. Chu), pan2@uakron.edu (E. Pan), jjr19@zips.uakron.edu (J.J. Ramsey), jxwang@pku.edu.cn (J. Wang), maryxue2010@gmail.com (C.X. Xue).

0020-7683/$ - see front matter © 2010 Elsevier Ltd. All rights reserved.
doi:10.1016/j.ijsolstr.2010.11.002

Different analytical or semi-analytical approaches based on Green's functions have also been developed to analyze the strain distributions in nanostructures (Nozaki and Taya, 1997; Downes et al., 1997; Pearson and Faux, 2000; Davies, 2003; Pan, 2004; Chu and Wang, 2005a,b; Wang et al., 2006; Even et al., 2007; Cheche and Chang, 2008; Liang et al., 2009). These approaches are typically less computationally expensive than numerical approaches such as FEM or BEM, but they also involve simplifying assumptions. One such assumption is to treat the material of the nanostructures (i.e. QWR or QD) as if it were the same as that of the surrounding matrix (Downes et al., 1997; Pearson and Faux, 2000; Davies, 2003; Pan, 2004; Chu and Wang, 2005a,b; Wang et al., 2006; Cheche and Chang, 2008), essentially treating a nanostructure problem as an Eshelby inclusion problem (Eshelby, 1957; Eshelby, 1959; Eshelby, 1961). Another common assumption, often used along with the previous one, is to neglect the anisotropy of the material in the system either totally (Downes et al., 1997; Pearson and Faux, 2000; Davies, 2003; Chu and Wang, 2005a,b; Cheche and Chang, 2008) or partially (e.g. by assuming the material is transversely isotropic (Even et al., 2007)) A more comprehensive review is given by Maranganti and Sharma (2007). The perturbation theory proposed in this paper releases the aforementioned simplifying assumptions.

The authors have previously used a perturbation theory to analyze purely elastic nanostructures (Wang and Chu, 2006). In this paper, we now present a generalized version of this theory so that it can be applied to inhomogeneous anisotropic piezoelectric structures. The structure analyzed here is three-dimensional, and the anisotropy of the materials, the difference between the material constants of the inhomogeneity and matrix, and the full coupling between elastic and electric fields are all considered in this theory. This paper is organized as follows. In the next section, the fundamental piezoelectric equations and the piezoelectric perturbation are derived. In Section 3, the elastic and electric fields induced by lattice mismatch in a truncated pyramidal InAs/GaAs QD structure are calculated by the proposed method. Numerical results show that anisotropy and inhomogeneity can have a significant influence on the elastic and electric fields. A good convergence is also demonstrated in this section. Conclusions are given in the last section.

2. Theory

Consider an arbitrarily shaped anisotropic inhomogeneity or QD, occupying region Ω, embedded in an infinite anisotropic piezoelectric matrix which occupies region $E^3-\Omega$, as shown in Fig. 1(a). Within the region Ω is a misfit strain field $\boldsymbol{\gamma}^*$ which may be induced by lattice mismatch or thermal mismatch. This problem is referred to as the original problem in the following. The stiffness tensors of the inhomogeneity or QD and the matrix are denoted by $\mathbf{C}^{\mathrm{QD}}$ and $\mathbf{C}^{\mathrm{M}}$, respectively.

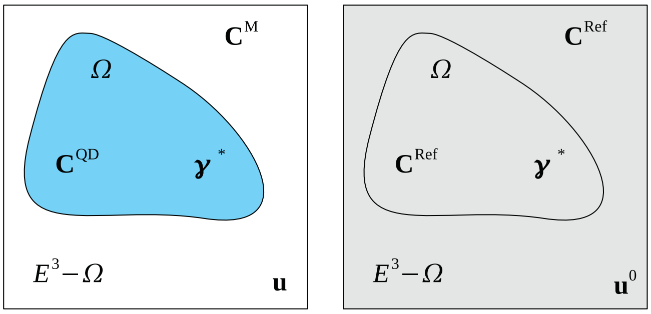

(a) (b)

Fig. 1. Schematics of (a) the original problem, an arbitrarily shaped anisotropic QD with lattice misfit strain $\boldsymbol{\gamma}^*$ in region Ω with material stiffness $\mathbf{C}^{\mathrm{QD}}$ embedded in an infinite anisotropic matrix with material stiffness $\mathbf{C}^{\mathrm{M}}$, and (b) the reference problem, an inclusion with material stiffness $\mathbf{C}^{\mathrm{Ref}}$ embedded in an infinite matrix under the action of an initial misfit strain prescribed in the inclusion region. The shape and size of the inclusion, and the misfit strain in the reference problem are the same as those in the original problem.

In order to solve this problem, a reference system composed of an Eshelby inclusion embedded in a matrix is introduced here. In the reference system, the material is an infinite, homogeneous medium with an eigenstrain field $\boldsymbol{\gamma}^*$ prescribed in a region Ω, as shown in Fig. 1(b). This is referred to as the reference problem in the following. The eigenstrain $\boldsymbol{\gamma}^*$ and the shape and size of the region Ω in the reference material are the same as those in the original one. Any body forces in the original and reference systems are identical as well. Since the reference material is homogeneous, the material constants inside and outside the region Ω are the same, and thus denoted by $\mathbf{C}^{\mathrm{Ref}}$. If piezoelectric effects are ignored, the reference problem is an Eshelby inclusion problem, which has been studied by many researchers (Eshelby, 1957; Eshelby, 1959; Eshelby, 1961; Mura, 1987; Melezhik and Korotchenkov, 2009). If the piezoelectric effects are considered, some useful results can be found in the references (Pan, 2002; Jiang and Pan, 2004; Pan, 2004; Wang et al., 2006; Even et al., 2007; Cheche and Chang, 2008; Kuvshinov, 2008). In this paper, we do not focus on how to solve the reference problem but on the original one. Therefore, the available methods for the reference problem will be used directly without detailed explanation.

In the Cartesian coordinate system, the constitutive relations of a piezoelectric material are

$$\begin{aligned} \sigma_{ij} &= C_{ijkl}(\gamma_{kl}-\gamma^*_{kl}) - e_{kij}E_k, \\ D_i &= e_{ijk}\left(\gamma_{jk}-\gamma^*_{jk}\right) + \varepsilon_{ij}E_j, \end{aligned} \tag{1}$$

where σ_{ij} denotes the stress and D_i the electric displacement. γ_{kl} denotes the strain and E_l the electric field. γ^*_{kl}, again, is the lattice mismatch strain, which is only nonzero within region Ω. C_{ijkl}, e_{ijk}, and ε_{ij} denote the elastic moduli, piezoelectric coefficients, and dielectric constants, respectively. Unless otherwise noted, lower case indices in this paper range from 1 to 3, while upper case indices range from 1 to 4. The summation conventions from 1 to 3 over repeated lower case indices and from 1 to 4 over repeated upper case indices are implied. The two expressions in Eq. (1) can be recast into:

$$\sigma_{iJ} = C_{iJKl}(\gamma_{Kl}-\gamma^*_{Kl}), \tag{2}$$

with

$$C_{iJKl} = \begin{cases} C_{ijkl} & J,K=j, \quad k=1,2,3, \\ e_{lij} & J=j=1,2,3; \quad K=4, \\ -e_{ikl} & J=4; \quad K=k=1,2,3, \\ \varepsilon_{il} & J=4; \quad K=4, \end{cases}$$

where $\sigma_{i4}=-D_i$, $\gamma_{4j}=-E_j$, and $\gamma^*_{4j}=0$. The governing equations of piezoelectric material become:

$$\sigma_{iJ,i}+f_J=0, \tag{3}$$

where f_k ($k=1,2,3$) denotes the kth-component of the body forces in the piezoelectric material, and $f_4=q$ denotes the electric charge density.

The constitutive relation in Eq. (2) can also be expressed in a matrix form, i.e.

$$\mathbf{T} = \begin{bmatrix} \mathbf{C}_{6\times6} & \mathbf{e}^{\mathrm{T}} \\ \mathbf{e} & \boldsymbol{\varepsilon}_{3\times3} \end{bmatrix}\mathbf{S} \equiv \mathbf{GS}, \tag{4}$$

with

$$\mathbf{T} = [\sigma_{11},\sigma_{22},\sigma_{33},\sigma_{23},\sigma_{13},\sigma_{12},-D_1,-D_2,-D_3]^{\mathrm{T}},$$

$$\mathbf{S} = [\gamma_{11},\gamma_{22},\gamma_{33},2\gamma_{23},2\gamma_{13},2\gamma_{12},E_1,E_2,E_3]^{\mathrm{T}},$$

$$\mathbf{e} = -\begin{bmatrix} e_{11} & e_{12} & e_{13} & e_{14} & e_{15} & e_{16} \\ e_{21} & e_{22} & e_{23} & e_{24} & e_{25} & e_{26} \\ e_{31} & e_{32} & e_{33} & e_{34} & e_{35} & e_{36} \end{bmatrix}, \quad \boldsymbol{\varepsilon} = -\begin{bmatrix} \varepsilon_{11} & & Sym \\ \varepsilon_{21} & \varepsilon_{22} & \\ \varepsilon_{31} & \varepsilon_{32} & \varepsilon_{33} \end{bmatrix},$$

where $\mathbf{C}_{6\times 6}$ is the elastic stiffness matrix. The matrix form of the constitutive relations is useful for numerical calculations.

The elastic displacements and electric potential for the original problem and the reference problem are u_I and $u_I^0 (I = 1, 2, 3, 4)$, respectively. For the QD region Ω of the original problem, substituting Eq. (2) into (3) yields:

$$C_{iJKl}^{\mathrm{QD}}\left(u_{K,li} - \gamma_{Kl,i}^*\right) + f_J = 0. \tag{5}$$

Similarly, for the region Ω in the reference problem:

$$C_{iJKl}^{\mathrm{Ref}}\left(u_{K,li}^0 - \gamma_{Kl,i}^*\right) + f_J = 0. \tag{6}$$

By subtracting Eq. (6) from Eq. (5), we get:

$$C_{iJKl}^{\mathrm{Ref}}\Delta u_{K,li} + \left(C_{iJKl}^{\mathrm{QD}} - C_{iJKl}^{\mathrm{Ref}}\right)\left(u_{K,li} - \gamma_{Kl,i}^*\right) = 0, \tag{7}$$

where $\Delta u_I = u_I - u_I^0$.

By a similar approach, we can get the corresponding equation for the matrix region, i.e.

$$C_{iJKl}^{\mathrm{Ref}}\Delta u_{K,li} + \left(C_{iJKl}^{\mathrm{M}} - C_{iJKl}^{\mathrm{Ref}}\right)u_{K,li} = 0. \tag{8}$$

The continuity condition of the elastic stress and electric displacement at the interface between the QD and the matrix in the original problem is

$$C_{iJKl}^{\mathrm{M}}u_{K,l}^+ n_i = C_{iJKl}^{\mathrm{QD}}\left(u_{K,l}^- - \gamma_{Kl}^*\right)n_i, \tag{9}$$

where n_i is the direction cosine of the unit normal vector to the interface and it points from the QD to the matrix. The superscripts '+' and '−' indicate that the physical quantities at the interface are on the matrix side and the QD side, respectively.

The continuity condition of the elastic stress and electric displacement at the interface in the reference problem is

$$C_{iJKl}^{\mathrm{Ref}}u_{K,l}^{0+} n_i = C_{iJKl}^{\mathrm{Ref}}\left(u_{K,l}^{0-} - \gamma_{Kl}^*\right)n_i. \tag{10}$$

By subtracting Eq. (10) from Eq. (9), we have:

$$\begin{aligned} C_{iJKl}^{\mathrm{Ref}}\Delta u_{K,l}^- n_i - C_{iJKl}^{\mathrm{Ref}}\Delta u_{K,l}^+ n_i = {} & \left(C_{iJKl}^{\mathrm{Ref}} - C_{iJKl}^{\mathrm{QD}}\right)\left(u_{K,l}^- - \gamma_{Kl}^*\right)n_i \\ & + \left(C_{iJKl}^{\mathrm{M}} - C_{iJKl}^{\mathrm{Com}}\right)u_{K,l}^+ n_i. \end{aligned} \tag{11}$$

Combining Eq. (7) with Eq. (8), while noting Eq. (11), it is observed that the difference of the elastic displacement and electric potential Δu_I can be treated as if they were the displacement and electric potential in the reference material due to effective body forces, f_J^1 and f_J^2, and an effective traction and charge density at the interface, T_J, where:

$$f_J^1 \equiv \left(C_{iJKl}^{\mathrm{QD}} - C_{iJKl}^{\mathrm{Ref}}\right)\left(u_{K,li} - \gamma_{Kl,i}^*\right) \quad \text{in } \Omega, \tag{12a}$$

$$f_J^2 \equiv \left(C_{iJKl}^{\mathrm{M}} - C_{iJKl}^{\mathrm{Ref}}\right)u_{K,li} \quad \text{in } E^3 - \Omega, \tag{12b}$$

$$\begin{aligned} T_J \equiv {} & \left(C_{iJKl}^{\mathrm{Ref}} - C_{iJKl}^{\mathrm{QD}}\right)\left(u_{K,l}^- - \gamma_{Kl}^*\right)n_i \\ & + \left(C_{iJKl}^{\mathrm{M}} - C_{iJKl}^{\mathrm{Ref}}\right)u_{K,l}^+ n_i \quad \text{at } \partial\Omega. \end{aligned} \tag{12c}$$

Hence, Δu_I can be easily expressed as

$$\Delta u_P = \int_\Omega G_{PJ} f_J^1 \mathrm{d}v + \int_{E^3-\Omega} G_{PJ} f_J^2 \mathrm{d}v + \int_{\partial\Omega} G_{PJ} T_J \mathrm{d}s, \tag{13}$$

where Ω and $E^3 - \Omega$ denote the QD region and the matrix region, respectively, and $\partial\Omega$ denotes the boundary of the QD, namely, the interface between the QD and the matrix. G_{PJ} denotes the Green's function for the homogeneous piezoelectric reference material with the modulus of C_{iJKl}^{Ref}. The above expression can be simplified by Gauss' theorem to give:

$$\begin{aligned} \Delta u_P = {} & -\int_\Omega G_{PJ,i}\left(C_{iJKl}^{\mathrm{Ref}} - C_{iJKl}^{\mathrm{QD}}\right)\left(u_{K,l} - \gamma_{Kl}^*\right)\mathrm{d}v \\ & - \int_{E^3-\Omega} G_{PJ,i}\left(C_{iJKl}^{\mathrm{Ref}} - C_{iJKl}^{\mathrm{M}}\right)u_{K,l}\mathrm{d}v. \end{aligned} \tag{14}$$

This formula can also be expressed in a compact form as

$$\Delta u_P = \int_{E^3} G_{PJ,i}\left(C_{iJKl} - C_{iJKl}^{\mathrm{Ref}}\right)\left(u_{K,l} - \gamma_{Kl}^*\right)\mathrm{d}v, \tag{15}$$

where $C_{iJKl} = C_{iJKl}^{\mathrm{QD}}$ in the QD region, and $C_{iJKl} = C_{iJKl}^{\mathrm{M}}$ otherwise. If we choose a reference material properly, such that $|\left(C_{iJKl}^{\mathrm{Ref}} - C_{iJKl}^{\mathrm{QD}}\right)\Delta u_{K,l}| \ll |C_{iJKl}^{\mathrm{Ref}}\Delta u_{K,l}|$, Eq. (15) can be approximated by

$$\Delta u_P \approx \int_{E^3} G_{PJ,i}\left(C_{iJKl} - C_{iJKl}^{\mathrm{Ref}}\right)\left(u_{K,l}^0 - \gamma_{Kl}^*\right)\mathrm{d}v. \tag{16}$$

Again, γ_{Kl}^* vanishes outside the QD region. The expression in Eq. (16) is an approximate result. If u_P^0 is called 0th-order approximate solution (0th-OAS), the new result $u_P^1 \equiv u_P^0 + \Delta u_P$ can be called the first-order approximate solution (1st-OAS). Obviously, based on the 1st-OAS and Eq. (15), we can get the 2nd-OAS, and so forth. Hence an iterative procedure is established.

If we choose the material of the matrix to be that of the reference problem, Eqs. (14) and (15) are simplified to the integral over Ω only as

$$\Delta u_P = \int_\Omega G_{PJ,i}\left(C_{iJKl}^{\mathrm{QD}} - C_{iJKl}^{\mathrm{M}}\right)\left(u_{K,l}^0 - \gamma_{Kl}^*\right)\mathrm{d}v. \tag{17}$$

If one compares Eqs. (16)–(17), it is apparent that the integration domain in the matrix has been reduced from E^3 to the smaller finite domain Ω. Thus, using the material property of the matrix as the reference material could substantially reduce the computation time during the numerical analysis.

3. An example

In this section, the elastic and electric fields in and around a truncated pyramidal InAs/GaAs QD (Lemaıtre et al., 2004; Adhikary et al., 2010), as shown in Fig. 2, are analyzed by the proposed method. The dimensions of this QD are: the side of the square base

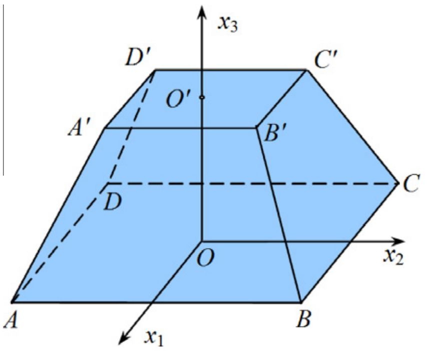

Fig. 2. Geometry of a truncated pyramidal QD InAs embedded in the GaAs matrix. In the numerical example, the upper and lower bases are both square with $AB = 12$ nm, $A'B' = 4$ nm. The height $OO' = 6$ nm. The initial nonzero lattice misfit strains are $\gamma_{11}^* = \gamma_{22}^* = \gamma_{33}^* = 6.9\%$.

Table 1
The piezoelectric constants of the InAs/GaAs QD structure and the selected reference material (Ref. Mat.). Since InAs and GaAs are cubic crystals, other constants can be obtained by the symmetry of the cubic crystal. Parameters C_{ij} are in GPa, while parameters e_{ij} are in C/m^2, and parameters ϵ_{ij} are in pF/m.

Material	C_{11}	C_{12}	C_{44}	e_{14}	ε_{11}
GaAs	118.8	53.8	59.4	0.160	110.7
InAs	83.3	45.3	39.6	0.0456	134.7
Ref. Mat.	130.0	30.0	50.0	0.	120.7

AB = 12 nm, the side of the upper base $A'B' = 4$ nm and the height $OO' = 6$ nm.

In the calculation, we select a reference material with its elastic isotropic constants and permittivity falling in between or near those of the real materials GaAs and InAs. For simplicity, we suppose there is no piezoelectric effect in the reference material, i.e. $e_{ijk} = 0$. It should be noted that the reference material is only a fictitious material. The material constants of GaAs, InAs and the reference material are listed in Table 1.

The initial misfit strains in InAs/GaAs QD are supposed to be induced by the lattice mismatch and can be calculated by the formula $(a_{\mathrm{InAs}} - a_{\mathrm{GaAs}})/a_{\mathrm{InAs}} \times 100\%$, where a_{InAs} and a_{GaAs} are the lattice constants of InAs and GaAs, respectively. Hence, $\gamma_{11}^{*} = \gamma_{22}^{*} = \gamma_{33}^{*} = 6.9\%$. The numerical results obtained by the proposed method are shown in Figs. 3–14.

For convenience in explaining the influence of the anisotropic properties on the elastic/electric fields and the convergence of the proposed method, we define the relative difference with respect to the second OAS as

$$\eta_{ii}^{j} = \left|\frac{\gamma_{ii}^{j} - \gamma_{ii}^{2}}{\gamma_{ii}^{2}}\right| \times 100\%, \quad (\text{no sum on } i) \tag{18a}$$

$$\zeta_{i}^{j} = \left|\frac{E_{i}^{j} - E_{i}^{3}}{E_{i}^{3}}\right| \times 100\%, \tag{18b}$$

where γ_{ii}^{j} and E_{i}^{j} denote the strain γ_{ii} and electric field E_i, respectively, for the jth-order approximate solution.

The distributions of the strains γ_{11}, γ_{22} and γ_{33} for zeroth, first and second order approximate solutions (OASs) along the line (x_1,0,3 nm) are shown in Figs. 3–5. Since the strains for third OAS nearly coincide with those for the second one, they are not given here. Due to the symmetry, the strains γ_{11} and γ_{22} at the point $(0,0,3\ \mathrm{nm})$ are equal. This phenomenon can be observed from the calculation results. For the zeroth OAS, they are both 6.29%; for the second OAS, 5.48%. The three strains γ_{11}, γ_{22} and γ_{33} all abruptly change at the interface and their absolute values inside the QD are larger than those outside the QD. The strains γ_{11} and γ_{33} get their maximum absolute values at the center $(0,0,3\ \mathrm{nm})$. The relative differences between the zeroth OAS and the second OAS at the center are $\eta_{11}^{0} = \eta_{22}^{0} \approx 15\%$ and $\eta_{33}^{0} \approx 17\%$. After one iteration, the differences decrease greatly, i.e. $\eta_{11}^{1} = \eta_{22}^{1} \approx 2\%$ and $\eta_{33}^{0} \approx 0.6\%$. The averages of the relative differences along the line from $(-4,0,3\ \mathrm{nm})$ to $(4,0,3\ \mathrm{nm})$ are about 12%, 16% and 22% for $\eta_{11}^{0}, \eta_{22}^{0}, \eta_{33}^{0}$, respectively. After one iteration, they decrease to 3.7%, 2.2% and 3.6%, respectively.

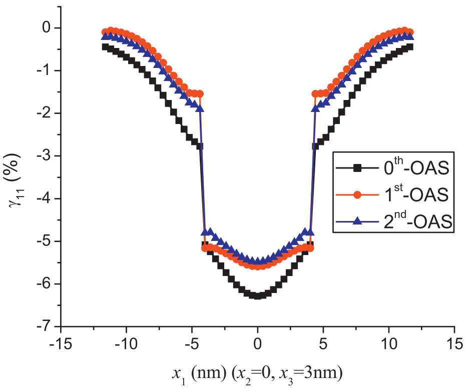

Fig. 3. Distribution of the elastic strain component γ_{11} along the line (x_1,0,3 nm) in the InAs/GaAs QD structure for different order approximate solutions. The initial lattice misfit strain is 6.9%.

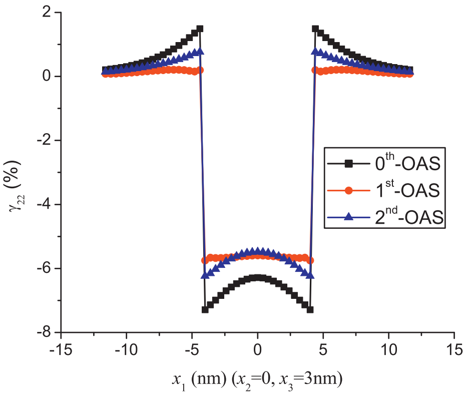

Fig. 4. Distribution of the elastic strain component γ_{22} along the line (x_1,0,3 nm) in the InAs/GaAs QD structure for different order approximate solutions. The initial lattice misfit strain is 6.9%.

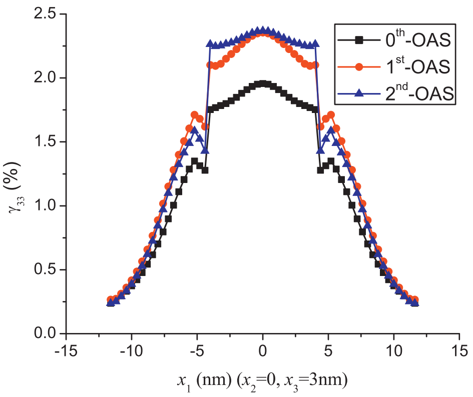

Fig. 5. Distribution of the elastic strain component γ_{33} along the line (x_1,0,3 nm) in the InAs/GaAs QD structure for different order approximate solutions. The initial lattice misfit strain is 6.9%.

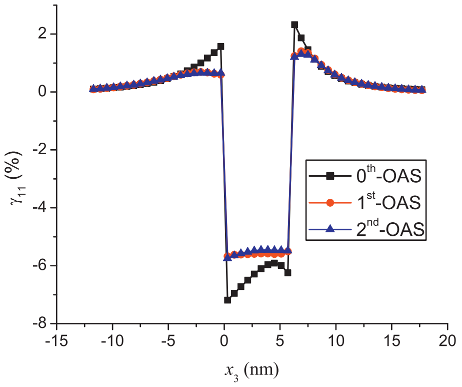

Fig. 6. Distribution of the elastic strain component γ_{11} along the x_3-axis in the InAs/GaAs QD structure for different order approximate solutions. The initial lattice misfit strain is 6.9%.

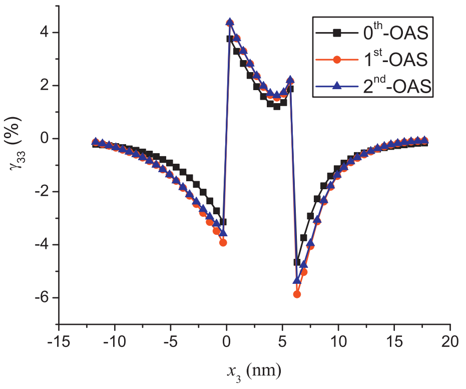

Fig. 7. Distribution of the elastic strain component γ_{33} along the x_3-axis in the InAs/GaAs QD structure for different order approximate solutions. The initial lattice misfit strain is 6.9%.

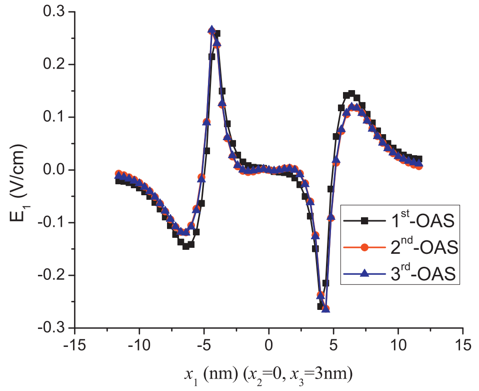

Fig. 8. Distribution of the electric field component E_1 along the line $(x_1, 0, 3\text{ nm})$ in the InAs/GaAs QD structure for different order approximate solutions. The initial lattice misfit strain is 6.9%.

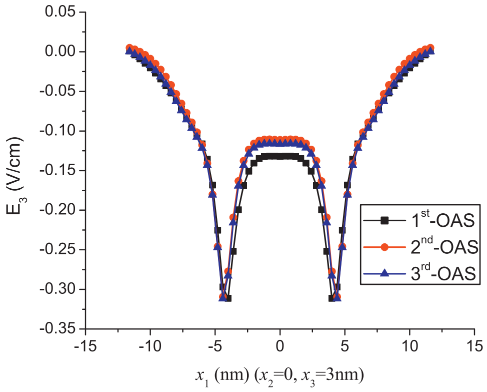

Fig. 9. Distribution of the electric field component E_3 along the line $(x_1, 0, 3\text{ nm})$ in the InAs/GaAs QD structure for different order approximate solutions. The initial lattice misfit strain is 6.9%.

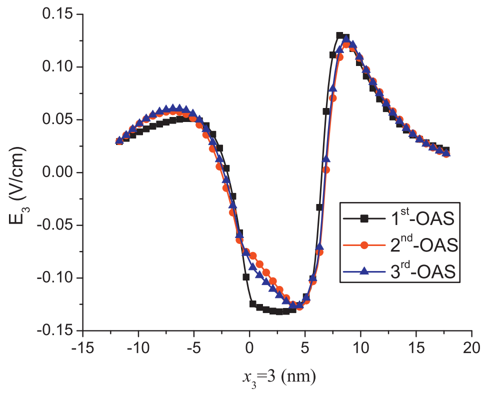

Fig. 10. Distribution of the electric field component E_3 along the x_3-axis in the InAs/GaAs QD structure for different order approximate solutions. The initial lattice misfit strain is 6.9%.

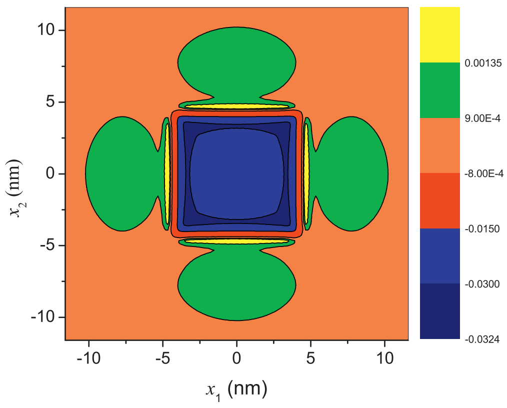

Fig. 11. Contours of hydrostatic strain on horizontal middle plane (x_3 = 3 nm) in the InAs/GaAs QD structure. The initial lattice misfit strain is 6.9%.

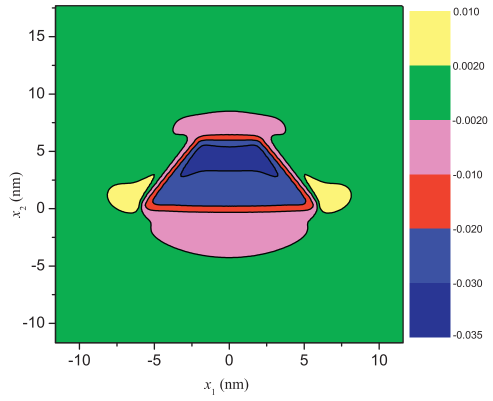

Fig. 12. Contours of hydrostatic strain on vertical middle plane (i.e. x_2–x_3 coordinate plane) in the InAs/GaAs QD structure. The initial lattice misfit strain is 6.9%.

Distributions of γ_{11} and γ_{33} along the x_3-axis for different OASs are shown in Figs. 6 and 7. The strain γ_{22} along the x_3-axis is always equal to γ_{11} due to the symmetry of the structure. Hence, it is not shown here. It is observed that strain fields have an abrupt change at the interfaces, i.e. $x_3 = 0$ and $x_3 = 6$ nm, and decrease rapidly with the increase of the distance from the QD. The two figures also show that the convergence of the iteration is very good, and the second OAS nearly coincides with the first one. The averages of the relative differences here are about 15% and 18%, respectively, for η_{11}^0 and η_{33}^0, and they decrease to 1.1% and 1.7%, respectively, after one iteration. The large difference between the zeroth OAS and the first/second one indicates that the anisotropic properties have a great influence on the elastic fields.

Distributions of electric fields E_1 and E_3 along the line $(x_1, 0, 3\text{ nm})$ and the distribution of E_3 along the x_3-axis are shown in Figs. 8–10. It should be noted that there are no electric fields for the 0th-OAS, since the reference material has no piezoelectric

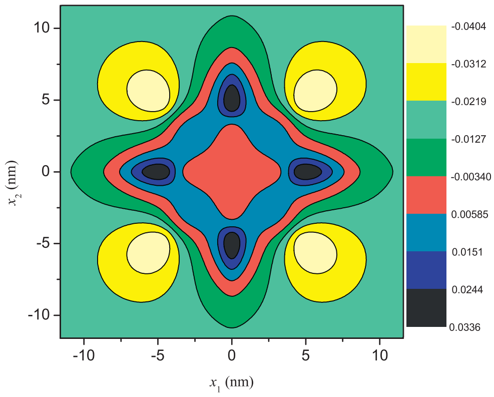

Fig. 13. Contours of electrical potential on horizontal middle plane (x_3 = 3 nm) in the InAs/GaAs QD structure. The initial lattice misfit strain is 6.9%.

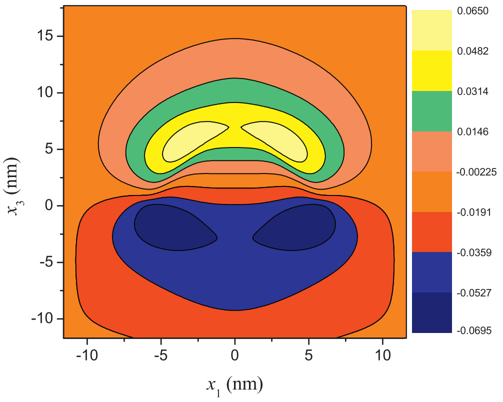

Fig. 14. Contours of electric potential on vertical middle plane (i.e. x_2–x_3 coordinate plane) in the InAs/GaAs QD structure. The initial lattice misfit strain is 6.9%.

coupling, i.e. $e_{ijk} = 0$. The electric field E_2 along the line (x_1,0,3 nm), and E_1 and E_2 along the x_3-axis are exactly zero. E_1 in Fig. 8 does not vary much inside the QD. Rather, the maximum difference $\triangle E = E_1^3 - E_1^1$ is 0.045 V/cm at x_1 = 5.2 nm, and its corresponding relative difference ζ_1^1 is about 53%. Unlike the results for E_1, the major difference among the first, second and third OASs of E_3 happens inside the InAs/GaAs QD, as shown in Figs. 9 and 10. It is observed from Fig. 10, the relative difference ζ_3^1 for E_3 at (0,0,3 nm) is about 13%. The average of ζ_3^1 along the line from (−4 nm,0,3 nm) to (4 nm,0,3 nm) is about 15% and decreases to 4.1% with one more iteration. From Fig. 10, it is noted that the average of ζ_3^1 for E_3 is about 14% at the central region of the QD, and the average of ζ_3^2 is about 4.1%. In general, it is observed that the third OAS of the electric field nearly coincides with the second one. Therefore, the convergence of iteration is demonstrated again.

Contours of the hydrostatic strain $\gamma_0 = (\gamma_{11} + \gamma_{22} + \gamma_{33})/3$ for the second OAS in the horizontal and vertical middle planes are shown in Figs. 11 and 12. Actually, we have also analyzed the hydrostatic strain of the zeroth OAS, and found that they are exact zero outside the InAs/GaAs QD and constant inside, which arises from the isotropic-homogenous assumption and is further consistent with theoretical results and previous reports (Downes et al., 1997; Pearson and Faux, 2000; Chu and Wang, 2005a,b). By considering the anisotropic and inhomogenous properties of the real InAs/GaAs QD structure, the nonzero region of hydrostatic strain is enlarged, as shown in Figs. 11 and 12. However, although the hydrostatic strain γ_0 is not exactly zero outside the real QD, it decreases rapidly with the increasing distance from the QD. For example, γ_0 is less than 0.14% when x_1 > 6 nm in Fig. 11. It can be also observed that the hydrostatic strains at the interface region are larger than those at the center or outside the QD. The maximum magnitude of the hydrostatic strain in Fig. 11 is about 3.2%.

The contours for the third OAS of the electric potential in the horizontal and vertical middle planes are given in Figs. 13 and 14. The potential at the point (0,0,3 nm) is assumed to be zero in our numerical analysis. The symmetry of the potential arises from the symmetry of the shape of the QD. Based on the results on the horizontal plane in Fig. 13, the potential reaches its maximum 0.034 V at the point (4.8,0,3 nm) which is outside the QD, and reaches its minimum −0.040 V at the point (5.2,5.2,3 nm). The density of contours near the interface, especially near the vertex is larger than that at other regions. This phenomenon indicates that the electric fields at these regions are large, which is consistent with previous results shown in Figs. 8–10.

From Figs. 3–7, the curves of strains of different OASs show the iteration procedure has very good convergence. As mentioned before, the curves of the strains of the 3rd-OAS, which are not shown here, nearly coincide with those of the 2nd-OAS. The large difference between the zeroth and the 2nd-OAS indicates that the anisotropy and inhomogeneity have a great influence on the elastic field, which in turn influences the electric fields. According to the results shown in Figs. 8–10, the differences of the electric fields between the 2nd-OAS and 3rd-OAS are small enough to be neglected, and therefore, 2nd-OAS provides a good result for both elastic and electric fields. It should be mentioned that the convergence of iteration can be influenced by many factors, such as the properties of the real materials, the properties of the reference material, and the shape of the QD. Hence, the convergence properties of the iteration may be different for different structures.

4. Discussion and conclusions

In this paper, a three-dimensional piezoelectric perturbation theory is presented to calculate the elastic and electric fields in QD nanostructures, based on a proposed reference material and its corresponding Green's function. In this theory, the influences of anisotropy, the differences in material properties between the QD and matrix, and piezoelectric effects are all considered. Numerical results for the InAs/GaAs QD nanostructure show that the elastic and electric fields are strongly influenced by the anisotropy of the QD structure and the differences between the material properties of the piezoelectric QD and matrix. It is demonstrated that both the strain and electric field in the InAs/GaAs QD structure obtained by the second-order approximate solution are accurate enough. Numerical results also show that the density of contours of the electric potential at and near the interface is much larger than in other regions.

Furthermore, this method is very general and is applicable to various piezoelectric inhomogeneities in nanostructures. The inhomogeneity can be in any geometric shape and, both the inhomogeneity and matrix can have any elastic or piezoelectric anisotropy.

Acknowledgements

This work was partially supported by the National Natural Science Foundation of China (10602050), Jiangsu Government Scholarship for Overseas Studies, North University of China, and the ASEE/SMART Fellowship program.

References

Adhikary, S., Halder, N., Chakrabarti, S., Majumdar, S., Ray, S., Herrera, M., Bonds, M., Browning, N., 2010. Investigation of strain in self-assembled multilayer InAs/GaAs quantum dot heterostructures. J. Cryst. Growth 312, 724–729.

Ambacher, O., Smart, J., Shealy, J.R., Weimann, N.G., Chu, K., Murphy, M., Schaff, W.J., Eastman, L.F., Dimitrov, R., Wittmer, L., Stutzmann, M., Rieger, W., Hilsenbeck, J.,

1999. Two-dimensional electron gases induced by spontaneous and piezoelectric polarization charges in N- and Ga-face AlGaN/GaN heterostructures. J. Appl. Phys. 85, 3222–3233.

Bandyopadhyay, S., Nalwa, H.S. (Eds.), 2003. Quantum Dots and Nanowires. American Scientific Publishers.

Beck, M.J., van de Walle, A., Asta, M., 2004. Surface energetics and structure of the Ge wetting layer on Si(100). Phys. Rev. B 70, 205337.

Benabbas, T., Androussi, Y., Lefebvre, A., 1999. A finite-element study of strain fields in vertically aligned InAs islands in GaAs. J. Appl. Phys. 86, 1945–1950.

Capellini, G., Seta, M.D., Busby, Y., Pea, M., Evangelisti, F., Nicotra, G., Spinella, C., Nardone, M., Ferrari, C., 2010. Strain relaxation in high Ge content SiGe layers deposited on Si. J. Appl. Phys. 107, 063504.

Cheche, T.O., Chang, Y.-C., 2008. Analytical approach for strain and piezoelectric potential in conical self-assembled quantum dots. J. Appl. Phys. 104, 083524.

Chu, H.J., Wang, J., 2005a. Strain distribution in arbitrarily shaped quantum dots with nonuniform composition. J. Appl. Phys. 98, 034315.

Chu, H.J., Wang, J.X., 2005b. An approach for calculating strain distributions in arbitrarily shaped quantum dots. Chin. Phys. Lett. 22, 667–670.

Cullis, A.G., Midgley, P.A. (Eds.), 2008. Microscopy of Semiconducting Materials 2007. Springer.

Davies, J.H., 2003. Elastic field in a semi-infinite solid due to thermal expansion or a coherently misfitting inclusion. J. Appl. Mech. 70, 655–660.

Downes, J.R., Faux, D.A., O'Reilly, E.P., 1997. A simple method for calculating strain distributions in quantum dot structures. J. Appl. Phys. 81, 6700–6702.

Duggen, L., Willatzen, M., Lassen, B., 2008. Crystal orientation effects on the piezoelectric field of strained zinc-blende quantum-well structures. Phys. Rev. B 78, 205323.

Eshelby, J.D., 1957. The determination of the elastic field of an ellipsoidal inclusion, and related problems. Proc. R. Soc. Lond. A 241, 376–396.

Eshelby, J.D., 1959. The elastic field outside an ellipsoidal inclusion. Proc. R. Soc. Lond. A 252, 561–569.

Eshelby, J.D., 1961. Elastic inclusion and inhomogeneities. In: Sneddon, I.N., Hill, R. (Eds.), Progress in Solid Mechanics, vol. 2. North-Holland, pp. 89–140.

Even, J., 2009. Symmetry analysis and exact model for the elastic, piezoelectric, and electronic properties of inhomogeneous and strained wurtzite quantum nanostructures. Appl. Phys. Lett. 94, 102105.

Even, J., Doré, F., Cornet, C., Pedesseau, L., Schliwa, A., Bimberg, D., 2007. Semianalytical evaluation of linear and nonlinear piezoelectric potentials for quantum nanostructures with axial symmetry. Appl. Phys. Lett. 91, 122112.

Faux, D.A., Howells, S.G., Bangert, U., Harvey, A.J., 1994. Strain relaxation in strained buried heterostructure lasers. Appl. Phys. Lett. 64, 1271–1273.

Feneberg, M., Lipski, F., Sauer, R., Thonke, K., Wunderer, T., Neubert, B., Brückner, P., Scholz, F., 2006. Piezoelectric fields in GaInN/GaN quantum wells on different crystal facets. Appl. Phys. Lett. 89, 242112.

Garg, R., Haxha, V., Migliorato, M.A., Hue, A., Srivastava, G.P., Hammerschmidt, T., 2009. Strain dependence of piezoelectric coefficients for pseudomorphically grown semiconductors. Microelectron. J. 40, 601–603.

Gates, T.S., Odegard, G.M., Frankland, S.J.V., Clancy, T.C., 2005. Computational materials: multi-scale modeling and simulation of nanostructured materials. Comput. Sci. Technol. 65, 2416–2434.

Heidemeyer, H., Denker, U., Müller, C., Schmidt, O.G., 2003. Morphology response to strain field interferences in stacks of highly ordered quantum dot arrays. Phys. Rev. Lett. 91, 196103.

Holý, V., Springholz, G., Pinczolits, M., Bauer, G., 1999. Strain induced vertical and lateral correlations in quantum dot superlattices. Phys. Rev. Lett. 83, 356–359.

Jiang, X., Pan, E., 2004. Exact solution for 2d polygonal inclusion problem in anisotropic magnetoelectroelastic full-, half-, and bimaterial-planes. Int. J. Solids Struct. 41, 4361–4382.

Johnson, H.T., Freund, L.B., 2001. The influence of strain on confined electronic states in semiconductor quantum structures. Int. J. Solids Struct. 38, 1045–1062.

Kurdi, M.E., Bertin, H., Martincic, E., de Kersauson, M., Fishman, G., Sauvage, S., Bosseboeuf, A., Boucaud, P., 2010. Control of direct band gap emission of bulk germanium by mechanical tensile strain. Appl. Phys. Lett. 96, 041909.

Kuvshinov, B.N., 2008. Elastic and piezoelectric fields due to polyhedral inclusions. Int. J. Solids Struct. 45, 1352–1384.

Lassen, B., Barettin, D., Willatzen, M., Voon, L.C.L.Y., 2008. Piezoelectric models for semiconductor quantum dots. Microelectron. J. 39, 1226–1228.

Lemaıtre, A., Patriarche, G., Glas, F., 2004. Composition profiling of InAs/GaAs quantum dots. Appl. Phys. Lett. 85, 3717–3719.

Liang, X.H., Wang, B., Liu, Y.L., 2009. Thickness effect of a thin film on the stress field due to the eigenstrain of an ellipsoidal inclusion. Int. J. Solids Struct. 46, 322–330.

Liao, X.Z., Zou, J., Cockayne, D.J.H., Leon, R., Lobo, C., 1999. Indium segregation and enrichment in coherent In$_x$ Ga$_{1-x}$ As/GaAs quantum dots. Phys. Rev. Lett. 82, 5148–5151.

Ma, Z., Holden, T., Wang, Z.M., Salamo, G.J., Malikova, L., Mao, S.S., 2007. Strain-induced electronic energy changes in multilayered InGaAs/GaAs quantum wire structures. J. Appl. Phys. 101, 044305.

Makeev, M.A., Yu, W., Madhukar, A., 2004. Atomic scale stresses and strains in Ge/Si(001) nanopixels: an atomistic simulation study. J. Appl. Phys. 96, 4429–4443.

Maranganti, R., Sharma, P., 2007. Strain field calculations in embedded quantum dots and wires. J. Comput. Theor. Nanosci. 4, 715–738.

Melezhik, E., Korotchenkov, O., 2009. Elastic fields of quantum dots in semi-infinite matrices: Green's function analytical analysis. J. Appl. Phys. 105, 023525.

Migliorato, M.A., Cullis, A.G., Fearn, M., Jefferson, J.H., 2002a. Atomistic simulation of In$_x$ Ga$_{1-x}$ As/GaAs quantum dots with nonuniform composition. Physica E 13, 1147–1150.

Migliorato, M.A., Cullis, A.G., Fearn, M., Jefferson, J.H., 2002b. Atomistic simulation of strain relaxation in In$_x$ Ga$_{1-x}$As/GaAs quantum dots with nonuniform composition. Phys. Rev. B 65, 115316.

Mura, T., 1987. Micromechanics of Defects in Solids, second revised ed. Martinus Nijhoff.

Nozaki, H., Taya, M., 1997. Elastic fields in a polygon-shaped inclusion with uniform eigenstrains. J. Appl. Mech. 64, 495–502.

Pan, E., 2002. Elastic and piezoelectric fields around a quantum dot: fully coupled or semicoupled model? J. Appl. Phys. 91, 3785–3796.

Pan, E., 2004. Eshelby problem of polygonal inclusions in anisotropic piezoelectric full- and half-planes. J. Mech. Phys. Solids 52, 567–589.

Pan, E., Han, F., Albrecht, J.D., 2005. Strain fields in InAs/GaAs quantum wire structures: inclusion versus inhomogeneity. J. Appl. Phys. 98, 013534.

Pan, E., Albrecht, J.D., Zhang, Y., 2007. Elastic and piezoelectric fields in quantum wire semiconductor structures – a boundary integral equation analysis. Phys. Status Solidi B 244, 1925–1939.

Pan, E., Zou, Y., Chung, P.W., Zhang, Y., 2009. Interlayer correlation of embedded quantum-dot arrays through their surface strain energy distributions. Phys. Rev. B 80, 073302.

Pearson, G.S., Faux, D.A., 2000. Analytical solutions for strain in pyramidal quantum dots. J. Appl. Phys. 88, 730–736.

Pyrz, R., 2008. Optical and piezoelectric properties of ZnO nanowires and functional polymer-based nanocomposites. In: Bell, J., Yan, C., Ye, L., Zhang, L. (Eds.), Frontiers in Materials Science and Technology, Advanced Materials Research, vol. 32. Trans Tech Publications, pp. 107–110.

Ramsey, J.J., Pan, E., Chung, P.W., 2008. Modelling of strain fields in quantum wires with continuum methods and molecular statics. J. Phys. Condens. Matter 20 (48), 485215.

Rodríguez-López, J.L., Montejano-Carrizales, J.M., Pal, U., Sánchez-Ramírez, J.F., Troiani, H.E., García, D., Miki-Yoshida, M., José-Yacamán, M., 2004. Surface reconstruction and decahedral structure of bimetallic nanoparticles. Phys. Rev. Lett. 92, 196102.

Romanov, A.E., Baker, T.J., Nakamura, S., Speck, J.S., 2006. Strain-induced polarization in wurtzite III-nitride semipolar layers. J. Appl. Phys. 100, 023522.

Sharma, P., Ganti, S., 2004. Size-dependent eshelby's tensor for embedded nano-inclusions in corporating surface/interface energies. J. Appl. Mech. 71, 663–671.

Shi, L., Xu, K., Xiong, K.L., Yang, H., Ni, J., 2009. Influence of the electronic states anisotropy on the band gap pressure coefficient of In$_x$ Ga$_{1-x}$ N alloys. J. Appl. Phys. 106, 113511.

Shih, H.Y., Chen, T.T., Chen, Y.C., Lin, T.H., Chang, L.W., Chen, Y.F., 2009. Size-dependent photoelastic effect in ZnO nanorods. Appl. Phys. Lett. 94, 021908.

Steiner, T.D. (Ed.), 2004. Semiconductor Nanostructures for Optoelectronic Applications. Artech House.

Wang, J., Chu, H.J., 2006. A perturbation theory for calculating strain distributions in heterogeneous and anisotropic quantum dot structures. J. Appl. Phys. 100, 053520.

Wang, X.-L., Voliotis, V., 2006. Epitaxial growth and optical properties of semiconductor quantum wires. J. Appl. Phys. 99, 121301.

Wang, C.Y., Denda, M., Pan, E., 2006. Analysis of quantum-dot-induced strain and electric fields in piezoelectric semiconductors of general anisotropy. Int. J. Solids Struct. 43, 7593–7608.

Widmann, F., Simon, J., Daudin, B., Feuillet, G., Rouvière, J.L., Pelekanos, N.T., Fishman, G., 1998. Blue-light emission from GaN self-assembled quantum dots due to giant piezoelectric effect. Phys. Rev. B 58, R15989–R15992.

Yang, J., 2006. A review of a few topics in piezoelectricity. Appl. Mech. Rev. 59, 335–345.

Yang, B., Pan, E., 2002. Elastic analysis of an inhomogeneous quantum dot in multilayered semiconductors using a boundary element method. J. Appl. Phys. 92, 3084–3088.

Zhang, X.Y., Gharbi, M., Sharma, P., Johnson, H.T., 2009. Quantum field induced strains in nanostructures and prospects for optical actuation. Int. J. Solids Struct. 46, 3810–3824.